Manipulating deformable linear objects
– Vision-based recognition of contact state transitions –

Frank ABEGG, Dominik HENRICH, and Heinz WÖRN

Institute for Process Control and Robotics (IPR),
Computer Science Department, University of Karlsruhe,
Kaiserstraße 12, D-76128 Karlsruhe, Germany,
e-mail: [Abegg | dHenrich | Woern]@ira.uka.de, http://wwwipr.ira.uka.de/~paro/

Abstract

A new and systematic approach to machine vision-based robot manipulation of deformable (non-rigid) linear objects is introduced. This approach reduces the computational needs by using a simple state-oriented model of the objects. These states describe the relation of the object with respect to an obstacle and are derived from the object image and its features. Therefore, the object is segmented from a standard video frame using a fast segmentation algorithm. Several object features are presented which allow the state recognition of the object while being manipulated by the robot.

1 Introduction

Todays industrial robots are mostly still controlled by precise control programs which do not allow the handling of shape changing deformable objects. To overcome this inflexibility, research has focussed on integrating sensor information into the robot control. Recently, video cameras have become one of the preferred robot sensors as they mimic the human sense of vision and allow non-contact measurement of the environment.

Up to now, many approaches realizing different tasks of a visually guided robotic system can be found in literature [Hutchinson96]. However, there are only few approaches concerning deformable objects, even though there are many important industrial tasks [Byun96]. One example task is the cabling of car door frames (Figure 1).

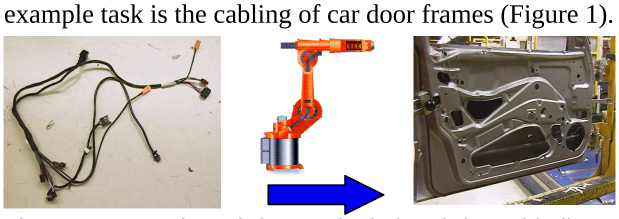

Figure 1: Example task for manipulating deformable linear objects: Cabling of car door frames.

The computational complexity of the recognition and the modeling of such dynamically changing objects let the deformable objects appear to be unfavorable for robot manipulation. Compared to the manipulation of rigid objects, some additional restrictions must be taken into consideration. The shape of a deformable object to be assembled is typically neither exactly known nor constant for the assembly process. While the initial shape depends on the history of the object, the deformation in the assembly process depends on contact forces and gravity. In addition, deformable objects have an inherent compliance which can hardly be influenced. Altogether, these effects cause high uncertainties which have to be dealt with. When using vision sensors, the overall complexity of computer vision processing is high and special lighting conditions are needed.

In this article, we formulate a general approach for the vision-based manipulation of deformable linear objects (DLO). The approach is used to implement task-independent manipulation primitives for industrial robots which can be combined for solving different tasks.

All known approaches to vision-guided handling of deformable linear objects so far only present a solution for one special problem. In [Chen91, Nakagaki96, Nakagaki97], a flexible beam is inserted into a drill. Nakagaki et al. additionally integrate a force/torque sensor while Chen et al. only use off-line sensor processing. In [Inoue83], a highly plastically deformable rope is used which is always hanging down and not deformed by a contact with an obstacle. Byun and Nagata compute the 3D pose of deformable objects but they have to deal with the stereo correspondence problem since they use a stereo vision approach [Byun96]. In the work of Smith, highly plastically deformable ropes are laid along a desired shape in a plane [Smith98] but non-elastic materials like ropes are not regarded in this work so far.

However, it is obvious that vision sensors are well-suited for observing characteristic shape changes of deformable objects. In that way, the information provided by vision sensors is complementary to that of other sensors as for example force/torque sensors. This is the reason why we use vision sensors together with a new approach in regarding deformable linear objects for robotic handling operations. This approach reported in [Remde99] serves as a base for most of the tasks concerning handling of deformable linear objects and reduces the computational needs by using a simple state-oriented model of such objects.

In the next section, a brief overview of this approach is given. The subsequent sections consider the questions: How can the approach be used together with a vision processing system for guiding a robotic handling system by observing the changes of the object shape (Section 3)?

How can the object be segmented from the image and which are the image features which can be used for state transition recognition of the object (Section 4)? What are the results in using our approach (Section 5)? What are the conclusions and how should the work be continued (Section 6)?

2 Basic Approach

In the following, the contact of a deformable linear object (called workpiece) in a static environment (called obstacle) is regarded. We base our consideration on the following two assumptions:

First, the material of the workpiece is isotrop and homogeneous. The workpiece is assumed to be *uniformly curved*, that is, it is either uniformly convex or concave. The deformation caused by gravity and contact forces is elastic, that is, the deformation removes if the stress is released.[1] Example workpieces are a (short) hose or a piece of spring steal. The linear workpiece is gripped at one end and the robot gripper may perform arbitrary linear motions.

Second, all obstacles consist of convex polyhedrons. The friction between workpiece and obstacle is negligibly low. We begin our consideration with a single contact between workpiece and obstacle.

Based on the geometric primitives of DLO and obstacle, a set of contact states is introduced which enumerates all possible contact situations [Henrich99]. For polyhedral objects, the geometric primitives are vertices (V), edges (E), and faces (F). The linear workpiece has two vertices and one edge between the two vertices. We name the contact states by the contact primitive of the workpiece followed by the contact primitive of the obstacle, for example V/F for vertex-face contact. An additional state is N which indicates that workpiece and obstacle are not in contact.

An important attribute of each contact state is its stability. A contact state which is kept up if the robot gripper performs a (small) motion in any direction is called *stable*. (However, the contact point or contact line may move). If this condition is not fulfilled, we call the contact state *unstable*. Consequently, a stable contact state is especially kept up if the robot gripper is not moved.

State transitions are a change from one contact state to another one without passing intermediate states. For now, establishing a second contact without loosening the first one, i.e., establishing a double contact, shall not be regarded. By combining the contact states with the transitions between them, the graph shown in Figure 2 is obtained. This graph gives all possible transitions between the contact states (including state N) and is found by means of basic manipulation experiments. Further details can be found in [Remde99].

In the next sections, the following two tasks are investigated: How can state transitions be detected with a machine vision system and what is necessary to perform the state transitions reliably and robustly with a robot system?

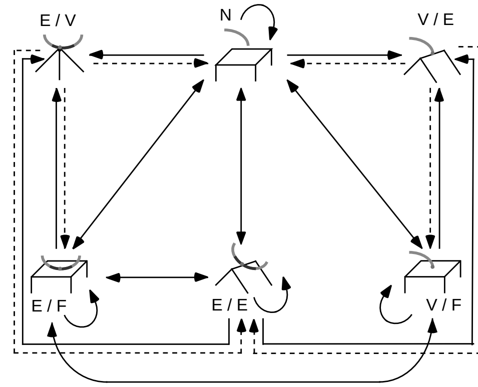

Figure 2: Contact state transition graph [Remde99] with initiated transitions (plain arrows) and spontaneous transitions (dashed arrows)

3 Vision-based workpiece manipulation

Since we believe that robust manipulation is possible without geometric reconstruction of the workpiece and the scene, a monocular camera system is used in order to observe the deformation of the workpiece. The deformation of the workpiece is detected by the change of several image features which are extracted from the workpiece shape in the image space. Since deformation can mean a change of the workpiece state in the context of the state model introduced in Section 2, changes of the image features of the workpiece and knowledge about the initial workpiece state are used to derive the current contact state as illustrated in Figure 3. Please note that the coarse obstacle geometry is a-priori given since it is assumed not to be changing and, therefore, can be easily given by the programmer or an environment data base.

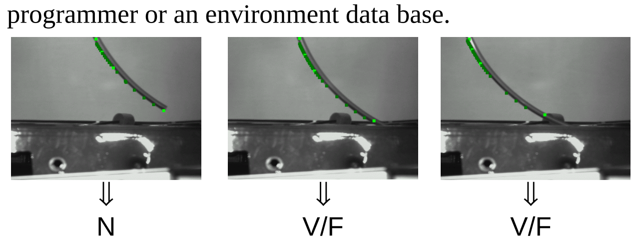

Figure 3: Recognition of workpiece states an image sequence

Based on the current state estimation, the robot is moved by a sequence of linear movement commands which have the aim to transfer the workpiece to a desired final state. Generally spoken, a feature-based visual robot control is built. The core of the control are task-independent sensori-motor primitives [Morrow95]. In this work, sensori-motor primitives control the state of the deformable workpiece. In general, these primitives have a controller-like structure as illustrated in Figure 4 and can be combined to task dependent robot operations like for example the threading of a workpiece through a hole.

---

[1] The workpieces belong to the object classes {E–, E+} introduced by [Henrich 99].

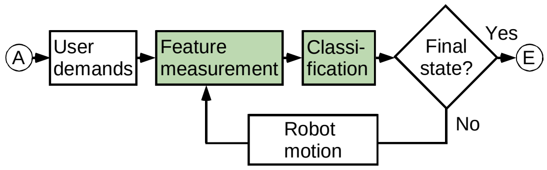

Figure 4: General structure of sensori-motor primitives with initial state (A) and final state (E)

In our context, sensori-motor primitives transfer a deformable workpiece from a given initial (A) stable contact state to another, desired contact state (E) with guarded robot moves: while the robot motion, the workpiece features are evaluated and used to recognize the current workpiece state. The next section describes the details of this feature extraction and Section 5 shows details of the recognition process.

4 State transition recognition

In order to get information about the shape of a deformable workpiece, it is necessary to extract the workpiece from the image of the scene. This is commonly known as segmentation. Here, it is assumed that the workpiece is observed from a stationary viewpoint where characteristic shape changes occur in the image.[2] After the segmentation, the deformable workpiece has to be characterized and so some features of the vision data have to be derived. Thus, we have to investigate in two areas: workpiece segmentation and feature extraction.

4.1 Workpiece segmentation

Since there is no need to extract the obstacles from the image and since we have a stationary camera, we are using a differential image method to get an idea where the main information about the deformable workpiece is. For that, the current image of the scene including the workpiece is subtracted from a reference image covering the scene without workpiece.

Assuming a nearly constant illumination, the image information is furthermore reduced by binarizing the current differential image which results in an image like Figure 5, left. The threshold for binarization is determined by taking a value near the mean gray value of the differential image. Even changing illumination can be allowed if the pixels not belonging to the workpiece of the differential image are taken as new reference image pixels.

Having now an image where the workpiece is segmented, the next step is to get a representation of the workpiece from which features can be derived which describe the deformation. In the case of linear workpieces, the curve of the projected shape is characteristic for the deformation state. Thus, data from the image of the workpiece

Unfortunately, even thin linear workpieces produce an image with several pixels of extension. In order to get a single curve the workpiece has to be thinned with thinning operations like in [Byun96]. Since thinning operations are time consuming iterative operations and tend to be not robust against perturbations in the image[3], we developed a new algorithm based on a contour following principle. The algorithm searches characteristic image points along the image border of the workpiece. The binarization has not to be made over the whole image, and thus, again we save time by performing the binarization locally while searching the contour.

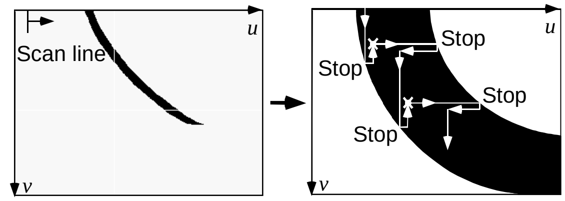

Figure 5: Principle of the contour following algorithm. Left: a binarized image. Right: the general principle of following the workpiece shape. An × marks a collected base point

The workpiece segmentation algorithm is illustrated in Figure 5. After the begin of the workpiece is found at any of the four image borders (indicated by the scan line in the figure), it searches in turn along the two image axes directions the border of the workpiece contour. The primary direction is orthogonal to the scan direction where the workpiece was first detected. The other direction becomes the secondary direction. For the example above, the primary direction is parallel to the v-axis (downwards) of the image and the secondary parallel to the u-axis (right).

Working with a vision sensor, perturbations usually disrupt the workpiece image in two or more regions. This causes the problem that the end of the workpiece would be suggested at the point of the first disruption where the binary value of the pixel changes. The algorithm solves this problem by starting a new local search for a possible further region within a look-ahead window. Within a segment and the window, the search is made fault tolerant against abrupt changes of the gray values of several pixels beyond the binarization threshold by using a finite state machine. For details see [Engel99].

While searching along these directions, the algorithm traverses the cable through rectangles in which the workpiece lies and which are called *segments*. The workpiece now is approximated by points which lie on the diagonals of these rectangles. With this method, it is possible to collect base points of the workpiece which have the same pixel distance. As distance value the Manhattan norm is used. Characteristic base points with different distances are already given by the corner points of the rectangles. Figure 9 shows a workpiece with detected base points.

---

2 Working in the image space allows us to change the camera position without needing a subsequent calibration process.

3 Thinning operations often have unconnected structures as result.

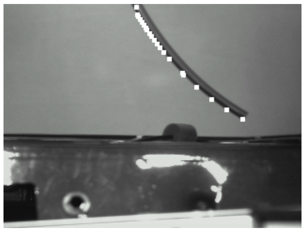

Figure 9: Detected cable base points (white dots)

The algorithm was validated in various experiments and works well under daylight and artificial lighting conditions. Measurements give a mean execution time of 1.1ms on an Intel Pentium machine with 133 MHz when a workpiece is detected. Problems occur when the robot moves into the image and is confused with the workpiece. This general problem with differential images can be solved by restricting the search space in the image.

4.2 Feature extraction

Having the base point list as a representation of the workpiece in the image, features are derived from this list which give hints to the contact state of the workpiece. These hints occur when the robot is manipulating. Thus, dynamic features are regarded. Remind that the initial and final workpiece state from the graph in Section 2 are given by the operator.

With a list of base points of the two-dimensional image space three types of characteristic features can be regarded. These are features concerning (1) the start or endpoint of the list, (2) one point within the list, or (3) the whole list of base points. The experiments show that features of type (1) and (3) give the best information about the workpiece state for one stationary camera.

The following list provides examples for these types of features which are fast computable:

- The pixel length $l(t)$ of the workpiece. Here, the length is the sum of the lines between the base points in pixels.
- The angle $a(t)$ between the line through the two endpoints and the image axis u, see Figure 10 left.
- The coordinates $p(t)=(u(t),v(t))$ of the endpoint not gripped are used for detecting changes of the contact state of the endpoint (Figure 10 left). Changes depend on the geometric relation of the workpiece and the workpiece endpoint.
- The tangent angle $g(t)$ in the endpoint indicates a change of the geometric relation between endpoint and obstacle. Figure 10 right shows a tangent between the endpoint and its preceding base point.
- The maximum curvature or the sum of curvatures $c(t) = \left(1/l(t)\right) \cdot \sum_{(u_i,v_i) \in base\ points(t)} k(u_i,v_i)$ where the curvature of a base point (u_i,v_i) is approximated by the discretization of the curvature k for regular curves f according to [Gray94]:

$$k(u_i,v_i) = \frac{\Delta f(u_i,v_i)\Delta^2 f(u_i,v_i) - \Delta^2 f(u_i,v_i)\Delta f(u_i,v_i)}{\sqrt[3]{\Delta f^2(u_i,v_i) + \Delta^2 f(u_i,v_i)}}$$

The first experiments reported in the next section show the applicability of this approach for robust state change detection when combining appropriate features.

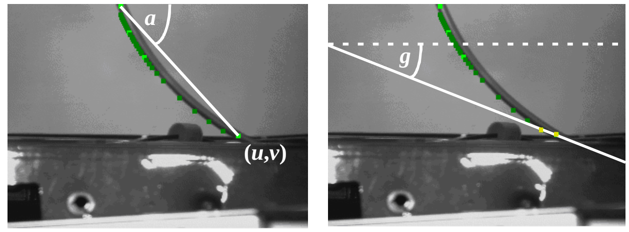

Figure 10: Endpoint angle a with respect to image axis u and endpoint coordinates u and v (left). Tangent angle g with respect to image axis u (right)

5 Experimental results

Based on the image features introduced in the last section, several experiments were performed in order to detect contact state transitions of the workpiece. At first, some manual manipulation experiments are presented. Then, some experiments with a robot and a stationary camera system are shown.

In the first experiment, a human grips a low elastic workpiece which belongs to the material class E- defined in [Henrich99], for example a pneumatic wire. Then, the workpiece behaves elastically under deforming forces greater than gravity. As obstacles for the manipulation, cubic and pyramidal objects are used similar to the objects shown in Figure 2. Then, each transition of the graph is examined by a human simulating a stationary monocular camera but with several different viewpoints. Furthermore, all transitions between two stable states with one unstable state in between are examined. For each transition, the human observes the workpiece features introduced in Section 4.2. When observing the features while a state change occurs, the change of the values of the (one-dimensional) features always can be designated to one of the characteristic feature changes A, B, C, D, E and F of Table 1. Examples for the feature changes are provided in Figure 11.

One next result is Table 2 in which all state changes that occur between two stable states are classified for four features.

Type	Properties
A	$\lvert\Delta f(t)\rvert < \varepsilon$
B	$\lvert\Delta f(t<t_0)\rvert > \varepsilon \ \wedge \ \lvert\Delta f(t>t_0)\rvert < \varepsilon$
C	$\lvert\Delta f(t<t_0)\rvert < \varepsilon \ \wedge \ \lvert\Delta f(t>t_0)\rvert > \varepsilon$
D	$0 \neq sign(\Delta f(t<t_0)) \neq sign(\Delta f(t>t_0)) \neq 0$
E	$\lvert\Delta f(t)\rvert > \varepsilon \wedge \lvert\Delta f(t<t_0) - \Delta f(t>t_0)\rvert > \varepsilon$
F	$\exists\delta>0:(\Delta^2 f(t_0-\delta<t<t_0)<-\varepsilon \ \wedge \ \Delta^2 f(t_0<t<t_0+\delta)>\varepsilon)$
	$\vee(\Delta^2 f(t_0-\delta<t<t_0)>\varepsilon \ \wedge \ \Delta^2 f(t_0<t<t_0+\delta)<-\varepsilon)$

Table 1: Properties of the characteristic feature changes based on threshold $\varepsilon > 0$

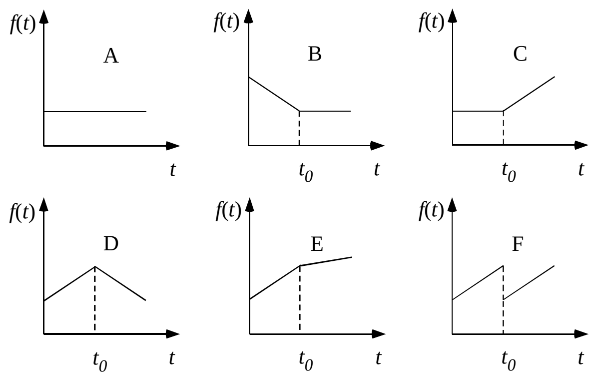

Figure 11: Examples for the observed characteristic changes of features $f(t)$. A: constancy, B: flatting out, C: change after constancy, D: roof/valley, E: slope change, F: jump

State transitions	Characteristic feature change for stationary vision observation $c(t)$	$p(t)$	$g(t)$	$a(t)$
N→V/F	C	B	C	C
N→E/E	C	D	C	C
N→E/F	C	D	C	C
V/F→N	B	C	B	B
V/F→E/F	B∨A	C∨A	B∨A	B∨A
V/F→V/E→N	F	F	F	F
V/F→V/E→V/F	E∨D	E∨D	E∨D	E∨D
V/F→V/E→E/E	E∨D	E∨D	E∨D	E∨D
E/E→N	B	B	B	B
E/E→E/F	B∨A	B∨A	B∨A	B∨A
E/E→V/E→N	F	F	F	F
E/E→V/E→V/F	E∨D	E∨D	E∨D	E∨D
E/E→E/V→N	F	F	F	F
E/E→E/V→E/E	E∨D	E∨D	E∨D	E∨D
E/E→E/V→E/F	E∨D	E∨D	E∨D	E∨D
E/F→N	B	B	B	B
E/F→V/F	A	B	A∨E	A
E/F→E/E	A	A	A	A
E/F→E/→VN	F	F	F	F
E/F→E/V→E/E	E∨D	E∨D	E∨D	E∨D
E/F→E/V→E/F	E∨D	E∨D	E∨D	E∨D

Table 2: Characteristic changes of features from Section 4.2 for each of the contact state transitions

Obviously, Table 2 shows that not every transition of the listed ones can be detected by observing only a single feature. A solution for that problem is to combine the information of multiple features in order to recognize a state transition of the cable workpiece. The recognition process can then be summarized as in Figure 12. Please note that additional process knowledge like the initial workpiece state is also needed. In the following, two experiments for this recognition process by machine vision processing are presented.

For the robot manipulation experiments, a Kuka KR15 robot is used. The robot controller executes motion commands sent from a Linux-PC with 350 MHz Pentium II Processor. As stationary camera, a standard video CCD-Camera (Hitachi KP M3) is used. The data are sent by a standard frame grabber to the vision processing computer which is a Linux-PC with 133 MHz Intel Pentium Processor. The gripped workpiece is a pneumatic polyurethane wire with outer diameter of 6 mm and a length of 300 mm. The obstacle is a car door frame which is mounted in a horizontal lying position.

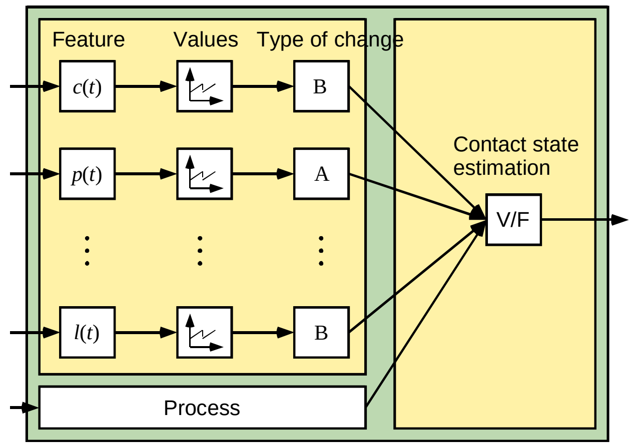

Figure 12: Summary of the recognition process

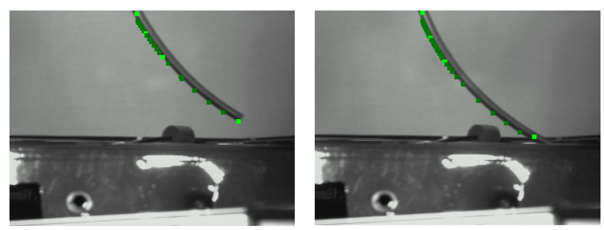

Figure 13: First and last image of a sequence where our robot is establishing a point contact with help of the feature information of the tracked workpiece

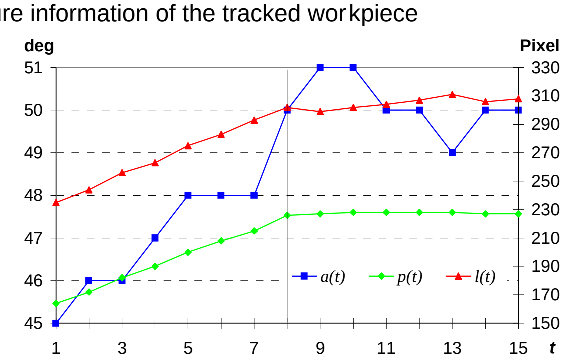

Figure 14: Diagram of three workpiece image features in a sequence with the starting and ending state shown in Figure 13 and the contact state transition N → V/F at t=8. ($a(t)$, $p(t)$, $l(t)$ according to Section 4.2)

Figure 13 shows two images of a sequence of images for a robot movement establishing a point contact on the flat car door frame: the non-contact state (left) and the established point contact (right). This contact establishment is denoted as a transition N→V/F in Figure 2. The first diagram in Figure 14 shows the values of three selected image features. Nearby the transition point, two of the curves, $p(t)$ and $a(t)$, show clearly the behavior of the type B of Table 1. The diagram in Figure 15 shows the curves of the same three features but for the transition V/F→V/E→N which is essential for the task of threading the workpiece through a hole. The transition sequence is established by moving the workpiece along the surface to the left towards a hole. The inner stress of the pneumatic wire is released when the endpoint reaches the hole. This transition is indicated best by the endpoint angle which makes a big leap. In such cases, our on-line transition recognition system realizes reliably this change and stops the robot motion.

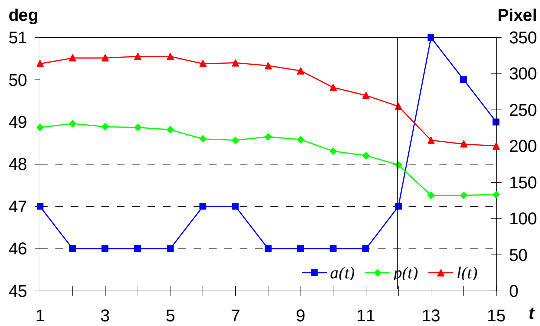

Figure 15: Diagram showing the curves for the same features like in Figure 14 but for the state transition V/F → V/E → N. V/E → N at time t=12

6 Conclusions and Future Work

Experimental results prove the applicability of our approach. Characteristic feature changes are derived from manual manipulation and observation experiments. These are used for implementation and optimization of the machine vision processing and the workpiece state classification. Two state transitions that are recognized reliably with our system are presented.

For future work, we have to investigate the question which parameters can be computed automatically and how can their number be minimized. This will also cover a robot hand-mounted camera and the comparison with the results for the stationary camera. Furthermore, we evaluate which general technology we can use for detection and classification of the workpiece state transitions. Our first choice will be classificators based on fuzzy logic. As further step, we will concatenate the implemented vision-based robot primitives for deformable linear objects in order to execute complex manipulation tasks.

Acknowledgements

The work is funded by the European Commission in the framework of the BriteEuram-project HANDFLEX (Integrated modular solution for HANDling of FLEXible materials in industrial environments). We want to thank the DaimlerChrysler AG, Germany, for supplying the cable forms.

References

[Byun96] Byun J.-E., Nagata T.: "Determining the 3-D pose of a flexible object by stereo matching of curvature representations". In: Pattern Recognition: The Journal of the Pattern Recognition Society, vol. 29, no. 8, pp. 1297-1308, 1996.

[Chen91] Cheng C., Zheng Y.F.: "Deformation identification and estimation of one-dimensional objects by using vision sensors". In: Proc. of the 1991 IEEE Int. Conf. on Robotics & Automation, Sacramento, California, USA, April, 1991.

[Engel99] Engel D.: "Entwicklung und Einsatz eines Algorithmus zur Segmentierung deformierbarer linearer Objekte aus stationär aufgenommenen Videobildern". One-term thesis, Institute for Process Control and Robotics (IPR), University of Karlsruhe, Germany, February 1999.

[Gray94] Gray A.: "Modern differential geometry of curves and surfaces", CRC Press, 1994.

[Henrich99] Henrich D., Ogasawara T., Wörn H. "Manipulating deformable linear objects – Contact states and point contacts". In: 1999 IEEE Int. Symp. on Assembly and Task Planning (ISATP'99), Porto, Portugal, July 21-24, 1999.

[Hutchinson96] Hutchinson S., Hager G.D., and Corke P.I.: "A tutorial on visual servo control". In: IEEE Trans. on Robotics and Automation, vol. 12, no. 5, October 1996.

[Inoue83] Inoue H., Inaba M.: "Hand-eye coordination in rope handling". In: Proc. of the First Int. Symp. On Robotics Research, pp. 163-174, New Hampshire, USA, September 1983.

[Morrow95] Morrow J.D., Khosla P.: "Sensorimotor primitives for robotic assembly skills". In: Proc. 1995 IEEE Int. Conf. on Robotics and Automation, pp. 1894-1899, Nagoya, Japan, May 1995.

[Nakagaki96] Nakagaki H., et al: "Study of insertion task of a flexible wire into a hole by using visual tracking observed by stereo vision". In: Proc. 1996 Int. Conf. on Robotics and Automation, vol. 4, pp 3209-3214, Minneapolis, MN, USA, April 22-28, 1996.

[Nakagaki97] Nakagaki H., Kitagaki K., Ogasawara T., Tsukune H.: "Study of deformation and insertion tasks of a flexible wire". In: Proc. of IEEE Int. Conf. on Robotics and Automation (ICRA'97), pp. 2397-2402, Albuquerque, USA, April 1997.

[Remde99] Remde A., Henrich D., Wörn H.: "Manipulating deformable linear objects - Contact state transitions and transition conditions". Submitted to: 1999 IEEE/RSJ Int. Conf. on Intelligent Robots and Systems (IROS'99), Kyongju, Korea, October 17-21, 1999.

[Smith98] Smith P.W.: "Image-based manipulation planning for non-rigid objects". In: Proc. 1998 Int. Conf. on Robotics and Automation, vol. 4, pp 3540-3545, Leuven, Belgium, May 1998.